Molecular Crystals and Liquid Crystals

ISSN: 1542-1406 (Print) 1563-5287 (Online) Journal homepage: http://www.tandfonline.com/loi/gmcl20

Phase Transitions and Molecular Mobility in 5CB and CE8 Studied by Dielectric Techniques

S. Kripotou, D. Georgopoulos, A. Kyritsis & P. Pissis

To cite this article: S. Kripotou, D. Georgopoulos, A. Kyritsis & P. Pissis (2015) Phase Transitions and Molecular Mobility in 5CB and CE8 Studied by Dielectric Techniques, Molecular Crystals and Liquid Crystals, 623:1, 407-423, DOI: 10.1080/15421406.2015.1066551

To link to this article: http://dx.doi.org/10.1080/15421406.2015.1066551

Published online: 21 Dec 2015.

Mol. Cryst. Liq. Cryst., Vol. 623: pp. 407–423, 2015

ISSN: 1542-1406 print/1563-5287 online
DOI: 10.1080/15421406.2015.1066551

Phase Transitions and Molecular Mobility in 5CB and CE8 Studied by Dielectric Techniques

S. KRIPOTOU, D. GEORGOPOULOS, A. KYRITSIS, AND P. PISSIS*

National Technical University of Athens, Department of Physics, Athens, Greece

Two complementary dielectric techniques, broadband dielectric relaxation spectroscopy (DRS) and thermally stimulated depolarization currents (TSDC), covering together broad ranges of frequency and temperature, were employed to study molecular mobility in the molecular liquid crystal 5CB. Three relaxations were observed and analyzed with respect to time scale, strength and shape, a sub-glass β relaxation and the α and δ relaxations in the supercooled nematic phase. In addition, TSDC and isochronal DRS measurements were used to follow phase transitions in 5CB and CE8 in comparison with DSC. The results demonstrate the power of dielectric techniques, in particular TSDC, for monitoring phase transitions in liquid crystals.

Keywords 5CB; CE8; molecular mobility; phase transitions; broadband dielectric relaxation spectroscopy; thermally stimulated depolarization currents

Introduction

Broadband dielectric relaxation spectroscopy (DRS) has been widely used for studying molecular dynamics in liquid crystals (LCs). References [1–4] are representative reviews, whereas references [5, 6] are representative for the corresponding theory.

Next to DRS, thermally stimulated depolarization currents (TSDC) is a powerful dielectric technique in the temperature domain [7]. This method consists of measuring the thermally activated release of stored dielectric polarization and it is characterized by high sensitivity and high peak resolving power. These characteristics, combined with the simplicity of the method and its low equivalent frequency [7], which enables to extend measurements to lower frequencies, not easily accessible by DRS, render TSDC to an attractive alternative, or better complementary, technique to DRS [8]. Nevertheless, in contrast to liquid crystalline polymers (LCPs), where TSDC has been widely used, references [9–12] being representative for that, only a few papers can be found in the literature on TSDC in molecular liquid crystals, as pointed out in [13]. Schober and Fischer employed TSDC to study orientational mobility of two molecular LCs, EBBA and MBBA, in their glassy nematic state [14]. Lacabanne and coworkers combined TSDC and DRS to study the α relaxation associated with the glass transition in a discotic LC [15]. In another study DRS and TSDC were employed to study molecular dynamics in a blend of a polyurethane

This paper was originally submitted to *Molecular Crystals and Liquid Crystals*, Volume 615, Proceedings of the 12th European Conference on Liquid Crystals.

*Address correspondence to P. Pissis, National Technical University of Athens, Department of Physics, Zografou Campus, 15780 Athens, Greece. E-mail: ppissis@central.ntua.gr

ionomer and a liquid crystalline oligomer [16]. Finally, reference [13] mentioned above deals with a detailed TSDC study of the α relaxation associated to the glass transition in 5CB.

In the present study we combine DRS and TSDC methods to study molecular mobility in a molecular liquid crystal, 4-n-pentyl-4′-cyanobiphenyl ($CH_3(CH_2)_4C_6H_4C_6H_4CN$, 5CB), over wide ranges of frequency and temperature. The phase behavior of 5CB is rather simple: it exhibits isotropic-nematic-solid mesomorphism, with transition temperatures around -35°C ($T_{I\text{-}N}$) and 20°C ($T_{N\text{-}S}$) for cooling rates of a few°C/min and a glass transition temperature of the supercooled nematic phase at about −70°C [17], compare DSC results later in this paper. The molecular structure of 5CB shown below

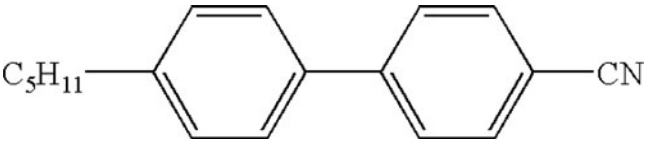

is characterized by the presence of a strong dipole moment along the long axis, which makes the material attractive for molecular dynamics studies by dielectric techniques and a model material for molecular LCs [18, 19].

Two processes have been observed in the supercooled nematic phase by dielectric techniques and investigated in several studies, a low-frequency process (in the following δ process) and a high-frequency process (in the following α process), assigned to reorientation of the molecule around its short axis and to different tumbling fluctuations of the molecule around its long axis, respectively [18]. By cooling at a sufficiently high rate, Drozd-Rzoska [19] was able to supercool the isotropic state and study in detail the α process associated with the glass transition. On the other hand, by combining DRS and heat capacity spectroscopy, Bras et al. [20] showed that in E7, which is a mixture of 5CB and three more molecular crystals, it is the dielectric tumbling mode (i.e. the α process) which has to be related to the dynamic glass transition. DRS was employed to study also the crystallization kinetics of isopentyl cyanobipheny, which is the chiral counterpart of 5CB, on heating the supercooled liquid [21]. In addition to neat 5CB, DRS was widely used, next to other techniques, to study effects on transitions and molecular mobility on mixing 5CB with benzene [22] or polystyrene [23] and on confining 5CB in nm pores [24–26]. To the best of our knowledge, no DRS study in 5CB was extended to lower temperatures to follow dynamics in the glassy state. In the present study, DRS measurements were performed in a broad temperature range down to -150°C and a secondary process in the glassy state was revealed and analyzed. Moreover, DRS and TSDC data were combined to provide a complete picture of dynamics over wide ranges of frequency and temperature in the LC under investigation.

In addition to studying molecular dynamics in detail, dielectric techniques are well suited for phase transition studies as complementary to thermal analysis techniques, in particular to differential scanning calorimetry (DSC), emphasizing in many cases specific aspects of a transition. Adachi and co-workers, for example, employed DRS to follow phase transitions in neat 5CB and 5CB blended with polystyrene [23]. TSDC, being a dielectric technique in the temperature domain, as well as sensitive to space charge distributions, is particularly suited for phase transition studies. In that respect, we would like to mention here the pioneering work by Costa Ribeiro, who observed that phase changes in dielectrics and liquids are accompanied by charge separation, if proceeding in an orderly fashion, and introduced the term thermodielectric effect for that, and by Gross, who developed a theoretical model for explaining that effect [27 and references therein]. In the present study, we further explore the prospects and limits of both DRS and, in particular, TSDC, for

phase transition studies in molecular LCs. To that aim, we employ also DSC in 5CB for direct comparison with the dielectric techniques. As mentioned above, the phase behavior of 5CB is rather simple. Therefore, we extend our studies by including a molecular LC with a complex phase behavior, CE8, and illustrate the power of TSDC for phase transition studies.

Experimental

Materials

Two commercially available liquid crystals were studied. 4-n-pentyl-4′-cyanobiphenyl (5CB) and 4-(2-methylbutyl) phenyl 4′-n-octylbiphenyl-4-carboxylate (CE8), both provided by Merck and used as received.

Differential Scanning Calorimetry (DSC)

DSC measurements were performed in the temperature range between 60 and −120°C by using DSC commercial equipment of TA Instruments, Q200. The sample (4-5 mg) was sealed in a Tzero hermetic pan and measured under nitrogen atmosphere. A rate of 10°C/min was used for all the thermal scans.

Thermally Stimulated Depolarization Currents Technique (TSDC)

For TSDC measurements [7] a Keithley 617 electrometer in combination with the Novocontrol Quatro Cryosystem were used. The sample was placed between two circular brass electrodes (14 mm diameter for 5CB, and 12mm for CE8) with a micro syringe, while the distance between the electrodes was adjusted by silica spacers of 50 μm thickness. The capacitor prepared was placed in a Novocontrol TSDC sample cell. The experimental protocol for 5CB was as follows. The sample was initially heated up to 60°C, in order to be in the isotropic phase, and then cooled down to the polarization temperature (T_p) with a rate of 10°C/min. A dc voltage of 50V was applied for 5min at T_p and the sample was subsequently cooled down to −120°C with a rate of 10°C/min. The voltage was turned off at −120°C and the sample was heated up to 60°C with a rate of 3°C/min, while the depolarization current was recorded. Measurements at different T_p were performed (40, 0, 20 and −55°C) in order to follow both dynamics and phase transitions. An analogous protocol was followed also for measurements on CE8 in the temperature range from 40 to 150°C. TSDC measurements were performed also without the application of an external field [28].

Dielectric Relaxation Spectroscopy (DRS)

For DRS measurements [29] the Novocontrol Alpha Analyzer in combination with a Novocontrol Quatro Cryosystem (temperature stability better than ±0.1°C) were used. The procedure followed for the preparation of the capacitor was the same as the one followed for TSDC measurements. Two experiments were performed for 5CB, A and B. In experiment A the sample was heated up to 60°C and then cooled down to −150°C at a rate of 10°C/min, while the signal was recorded at four different frequencies (1MHz, 100-10-1KHz), in order to follow phase transitions. The sample was then measured during heating isothermally from −150 to 60°C in the frequency range from 10^{-1} to 10^6 Hz, in order to follow the

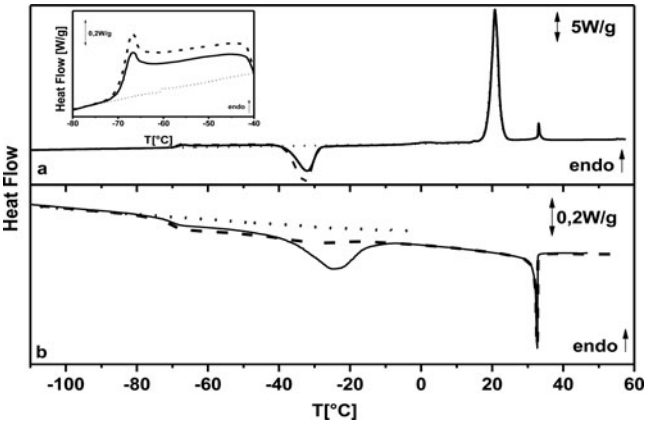

Figure 1. DSC thermograms during heating (a) and cooling (b) at a rate of 10°C/min. Solid lines: cooling from 50°C and subsequent heating up to 60°C. Dashed lines: cooling from 60°C/min and subsequent heating up to 0°C. Dotted lines: after complete crystallization of the sample and subsequent heating up to 60°C. The inset shows in magnification heating thermograms in the glass transition region.

relaxational behavior, with measurements every 10°C from −150° to −70°C, every 2°C from -64 to −40°C and every 5°C from -30 to 60°C. In experiment B the sample was initially heated up to 60°C and measured during cooling isothermally from 60°C to −150°C (every 5°C from 60°C to −10°C, every 2°C from −12°C to −56°C and every 10°C from −60°C to −150°C), again in the frequency range from 10^{-1} to 10^{6} Hz, in order to follow relaxations during cooling and to compare with heating [21].

No special treatment was employed for completely aligning the sample during dielectric measurements throughout this work, such as application of a dc bias field or use of polyimide foils between the sample and the brass electrodes, so the preferable orientation of the molecules is that perpendicular to the surface.

Results and Discussion

Phase Transitions – DSC

The thermal behavior of 5CB has been already studied, see for example [11, 17–19]. Here DSC measurements were performed in order to characterize the sample using the same thermal treatment as in dielectric measurements and, thus, enable direct comparison. By cooling the sample from 50 or 60°C at a rate of 10°C/min down to −120°C (Fig. 1b) a transition from the isotropic to a nematic phase is observed as a sharp exothermic peak at 32.7°C. Subsequent cooling of the sample results in partial crystallization (exothermic peak at −25°C). Interestingly, crystallization is more pronounced during the first cooling of the sample, an observation worth to be further followed in future work by non-isothermal and isothermal measurements [21, 30]. At lower temperatures, around −70°C, transition from the nematic liquid to the nematic glassy state is observed (at the cooling rate used [13, 19]). During subsequent heating of the sample (Fig. 1a), transition from glassy to liquid phase is observed as a step like increase in heat flow. A glass transition temperature T_g of

−71°C was calculated for the sample (fictive temperature). At about 40°C higher than the glass transition temperature, the sample crystallizes during heating (cold crystallization, exothermic peak at −32°C). On further heating, the sample goes from crystalline to nematic phase at 21°C (endothermic peak) and finally to the isotropic at 33°C (endothermic peak). When the sample is measured in the region of the glass transition after completion of cold crystallization at −32°C (dotted line Fig. 1), no glass transition is observed, indicating that the sample is in fact completely crystallized. So, according to the DSC results, when 5CB is cooled at a rate of 10°C/min, the sample is in the isotropic phase for T>33°C and in the nematic phase for −25°C<T<33°C, whereas it behaves like a supercooled nematic liquid having a small fraction of crystallites for T<-25°C with T_g = -71°C. During heating 5CB behaves like a supercooled nematic liquid (with $T_g = -71$°C) up to −32°C, it is completely crystalline for −32°C<T< 21°C (as indicated also by the invariance of the melting enthalpy for the various thermal histories in Fig. 1a), it is in the nematic phase for 21°C<T<33°C, and finally in the isotropic phase for T>33°C.

Phase Transitions - DRS

Figure 2 shows results of DRS measurements as a function of temperature during cooling and subsequent heating [23]. During cooling from isotropic phase a frequency independent increase of ε' and a discontinuity in ε'' is observed at 35°C (vertical dashed line) indicating the transition of the sample from the isotropic to the nematic phase (Fig. 2 a and b). At lower temperatures two frequency dependent step-like changes in ε' and a double peak in ε'', shifting to lower temperatures with decreasing frequency, which correspond to two dielectric relaxations, are observed. The relaxations will be analyzed in a next section. When the sample is heated up, it is in the same phase as during cooling (amorphous nematic phase) up to −50°C (vertical solid line), where crystallization occurs, as indicated by the frequency independent change in ε' (inset in Fig. 2a) and in ε'' (Fig. 2b). For higher temperatures and up to 20°C a constant low value of ε' is recorded, while no peaks can be followed in ε''. The sudden increase in ε' at 20°C (vertical solid line) indicates the transition from the crystalline to the nematic phase, while the subsequent decrease at 35°C indicates the transition to the isotropic phase. Adachi and coworkers performed similar measurements, following a different thermal protocol, slow cooling and heating (0.1°C/min) [23]. They pointed out the coexistence of phase transitions and relaxations in the temperature/frequency ranges of measurements, A discrepancy observed in the ε' values in the nematic phase between cooling and heating scans (not seen here), was assigned to changes in the orientation of the molecules with respect to the electrodes [23].

Dielectric transition temperatures determined from the changes in ε' and in ε'', especially for the transition from the isotropic to nematic (cooling) and from nematic to isotropic (heating), are in very good agreement with those determined by DSC.

Phase Transitions - TSDC

Figure 3 shows results of TSDC measurements (TSDC thermograms) for a 5CB sample polarized at different temperatures (T_p) to follow dynamics and phase transitions. For reasons of clarity results are shown separately in the temperature regions of the α relaxation (a), cold crystallization (b) and C-N and N-I transitions (c). The segmental α relaxation, associated with the glass transition, is followed in Fig. 3a. The peak temperature T_m of a TSDC α peak is a good measure of the calorimetric T_g [7], as confirmed also by the present

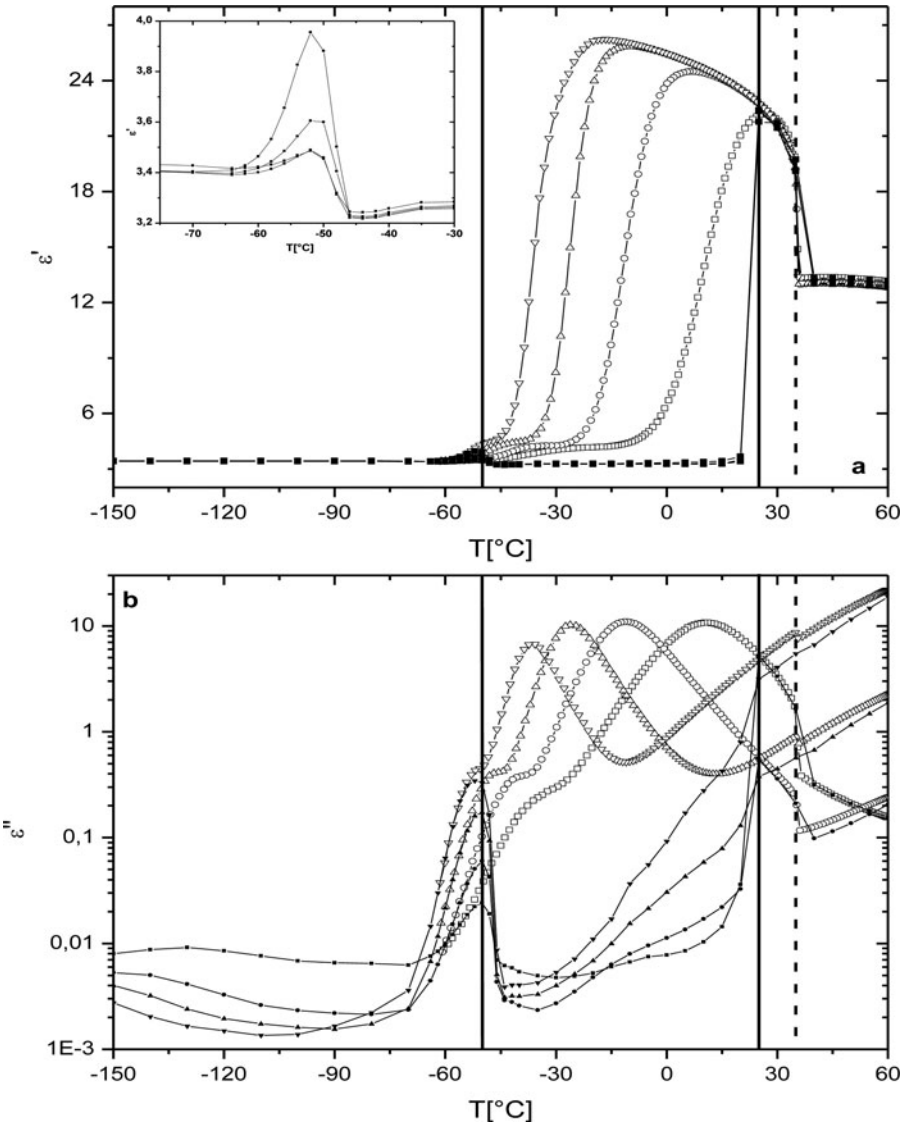

Figure 2. Real and imaginary part of dielectric function, ε' and ε'' as a function of temperature, in a and b, respectively, for 5CB between brass electrodes. Open symbols correspond to continuous cooling at a rate of 10°C/min and full symbols to heating remaining at each temperature for a frequency scan (12min). Different symbols correspond to different frequencies. Squares: 1MHz, Circles: 100kHz, Up Triangles: 10kHz, and Down Triangles: 1kHz. The inset shows a magnification in the region of cold crystallization during heating. Vertical lines are to guide the eye, details in text.

results ($T_g = -71°C$, $T_m = -67°C$), in agreement also with results of a detailed study of the TSDC α peak in 5CB [13]. T_m is practically independent from T_p. The contribution $\Delta\varepsilon$ of the α process to the static permittivity, calculated from the area under the peak [7], given on the plot, remains unchanged as long as the peak is fully polarized (in the isotropic

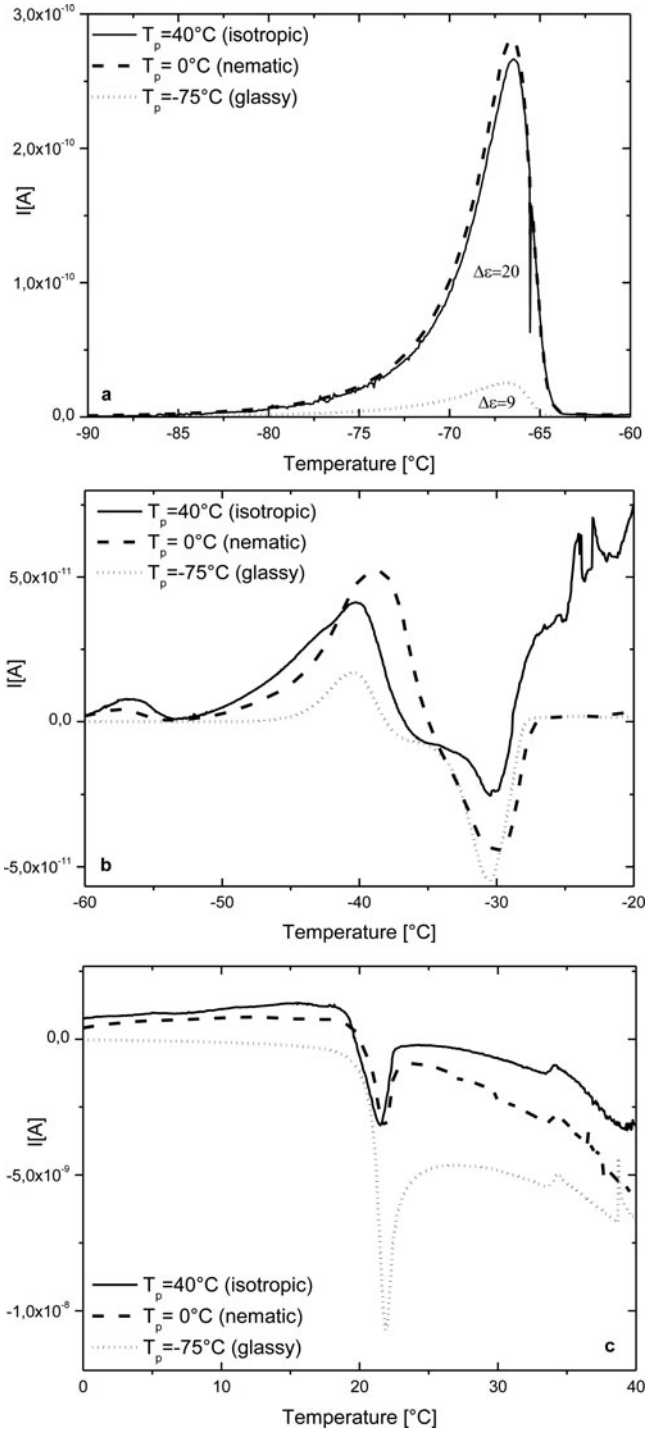

Figure 3. TSDC thermograms for 5CB between brass electrodes polarized at different temperatures (in different phases) indicated on the plot in the region of the α relaxation (a), cold crystallization (b) and C-N and N-I transitions (c).

and the nematic phases), whereas it decreases for partial polarization in the glassy state [7, 8]. The results for the time scale (T_m) and the strength of the α process will be further discussed in relation to DRS measurements in the next sections.

In Fig. 3 b and c we follow cold crystallization as a change of sign of the depolarization current, the C-N transition as a pronounced negative peak and the N-I transition as a small negative peak, with a high reproducibility of the temperature position, the shape and the size of the signals. The double peak in the temperature range of cold crystallization is of particular interest, as very often the TSDC α peak in glass forming liquids and polymers is followed by a (positive) peak related to conductivity, the so-called ρ peak [7]. However, the signal recorded in Fig. 3b in the region of cold crystallization is not a ρ peak, as confirmed by the appearance of the signal also at a much lower polarization temperature ($T_p = -75^\circ C$ in the glassy state) and by similar DSC-TSDC results in a different system, poly(dimethyl siloxane)/silica nanocomposites [31].

The significance of the TSDC results presented above is twofold, on the one hand for further studying and better understanding the thermodielectric effect [27] and on the other hand for establishing alternative techniques for phase transition studies (which, in addition, might be more sensitive than DSC for particular transitions). To further follow these points we present in Fig. 4 TSDC thermograms for another liquid crystal, CE8, with a much more complex phase behavior as measured by DSC: C - SmX (48°C) – SmG (61°C) – SmI (67°C) – SmC (70°C) – SmA (87°C) – N (135°C) – I (140°C) [17, 32]. For reasons of clarity results are presented separately at lower (a) and higher temperatures (b). Sharp peaks are detected in the temperature region of the first four transitions, also without applying a polarizing field [28], although of smaller intensity in that case, whereas the three higher temperature transitions are reflected as less clear changes in the shape of the response. The latter is probably related with higher conductivity, partly because of the higher temperature of the transitions, which overlaps with the signal coming from the transition, and points to limitations of the technique.

Molecular Mobility - DRS

Figure 5 shows results of isothermal DRS measurements during heating (experiment A, see section Experimental, DRS), imaginary and real part of dielectric function, ε'' (a) and ε' (b), respectively. At low temperatures we follow a weak relaxation (ε''_{max} at about 3×10^{-3}) in the glassy state, shifting rather slowly to higher frequencies with increasing temperature, located at about 10^2 Hz at -80°. To the best of our knowledge, this relaxation (called β relaxation in the following) has never been reported before in 5CB, where the focus was always at higher temperatures in the nematic and isotropic phases. Results to be reported below suggest that this is a secondary Johari-Goldstein β relaxation, characteristic of rigid molecular glass formers [33, 34]. At higher temperatures, in the supercooled nematic phase, a strong relaxation (ε''_{max} at about 3) enters into the frequency range of measurements, located at $10^{-1}-10^0$ Hz at -60°. At this temperature, a shoulder is discerned at higher frequencies, which becomes a clear peak at higher temperatures, -50° and -48°. The two peaks shift rapidly to higher frequencies with increasing temperature. At temperatures higher than -50° the intensity of the peaks decreases significantly (compare the graph at -46°C) and the peaks disappear already at -44°C, obviously because of cold crystallization (which occurs now at lower temperatures compared to DSC and TSDC, because of the different thermal history of isothermal DRS measurements). Only a weak relaxation can be followed at temperatures higher than about -45°C, in the temperature/frequency region of the β relaxation, which will be analyzed in the next section. The two loss peaks correspond

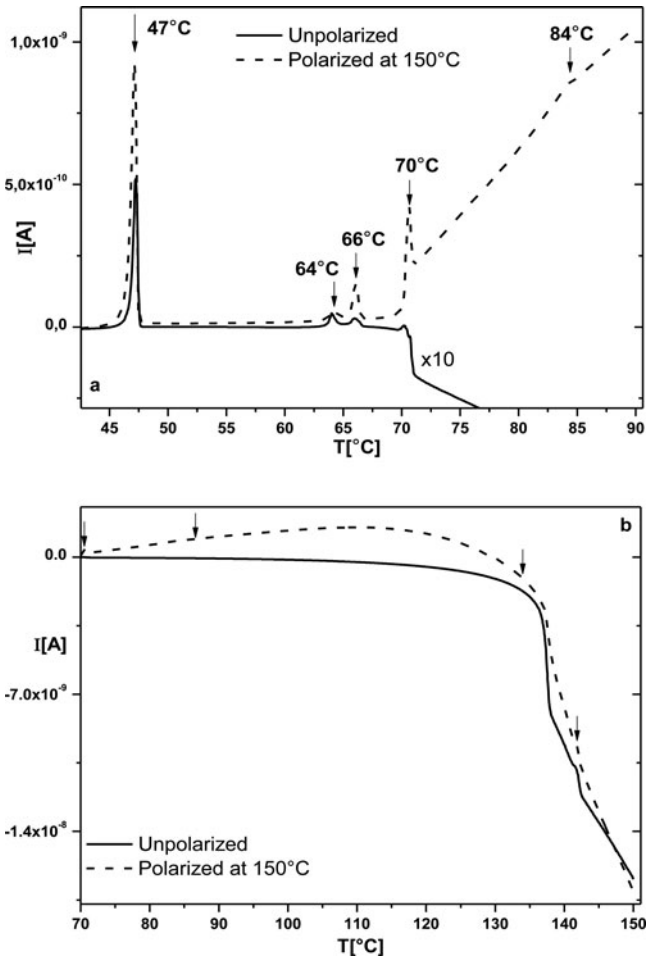

Figure 4. TSDC thermograms for CE8 between brass electrodes at lower (a) and higher temperatures (b) without applying voltage (unpolarized, solid line) and by applying 50V at 150°C (polarized, dashed line). The data for the unpolarized sample have been multiplied by 10.

to the δ and α relaxations, in the order of increasing frequency, studied already by several investigators [18–26] and assigned to reorientation of the 5CB molecule around its short axis and to different tumbling fluctuations of the molecule around its long axis, respectively. It is clear already in the raw data and will be confirmed by analysis that the δ process is narrower and of higher intensity than the α process. The two relaxations can be followed, obviously less clearly, also in the ε'(f) plots of Fig. 5b. At higher temperatures, conductivity dominates the response (steep increase of ε'' at low frequencies) and it is possible to follow the C-N transition as a sharp increase of conductivity and of ε' at 25°C and the N-I transition as a sharp decrease of ε' at 40°C.

In order to follow the α and δ relaxations at higher frequencies and temperatures (prohibited during heating due to crystallization), we performed isothermal measurements during cooling from 60 to −150°C, in steps of 5°C from 60 to −10°C, of 2°C from −12°C to −56°C, and of 10°C from −60°C to −150°C (experiment B). The data for

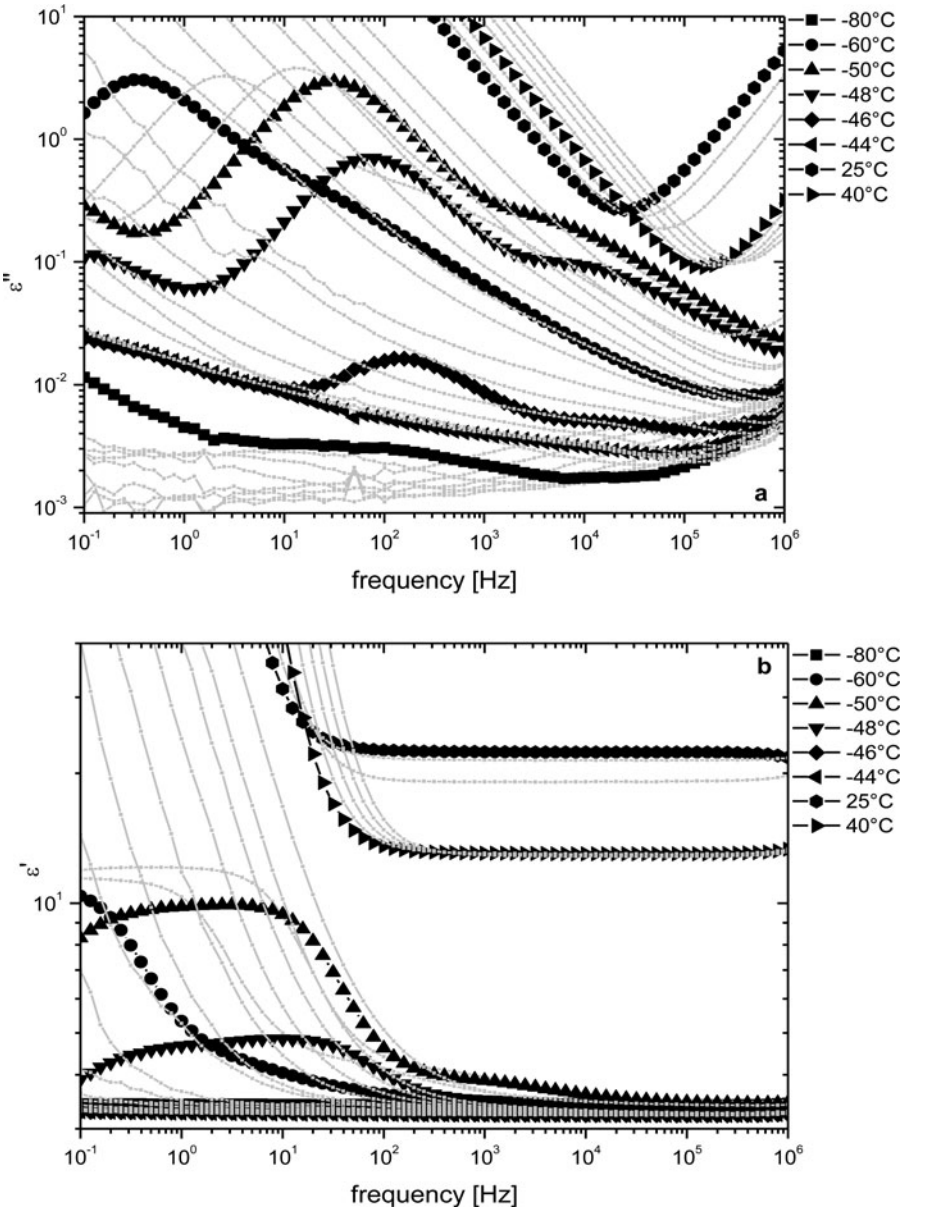

Figure 5. Imaginary and real part of dielectric function, ε'' and ε', as a function of frequency in a and b, respectively, at different temperatures, some of them indicated on the plots, for 5CB during heating (experiment A)

the imaginary and the real part of dielectric function are presented in Figure 6, a and b respectively. At temperatures lower than about 0°C a relaxation enters into the frequency range of measurement at high frequencies (step in ε' and peak in ε''), shifting to lower frequencies with decreasing temperature. The magnitude seems to decrease slowly with decreasing temperature (compare, however, the results of analysis in the next section), then

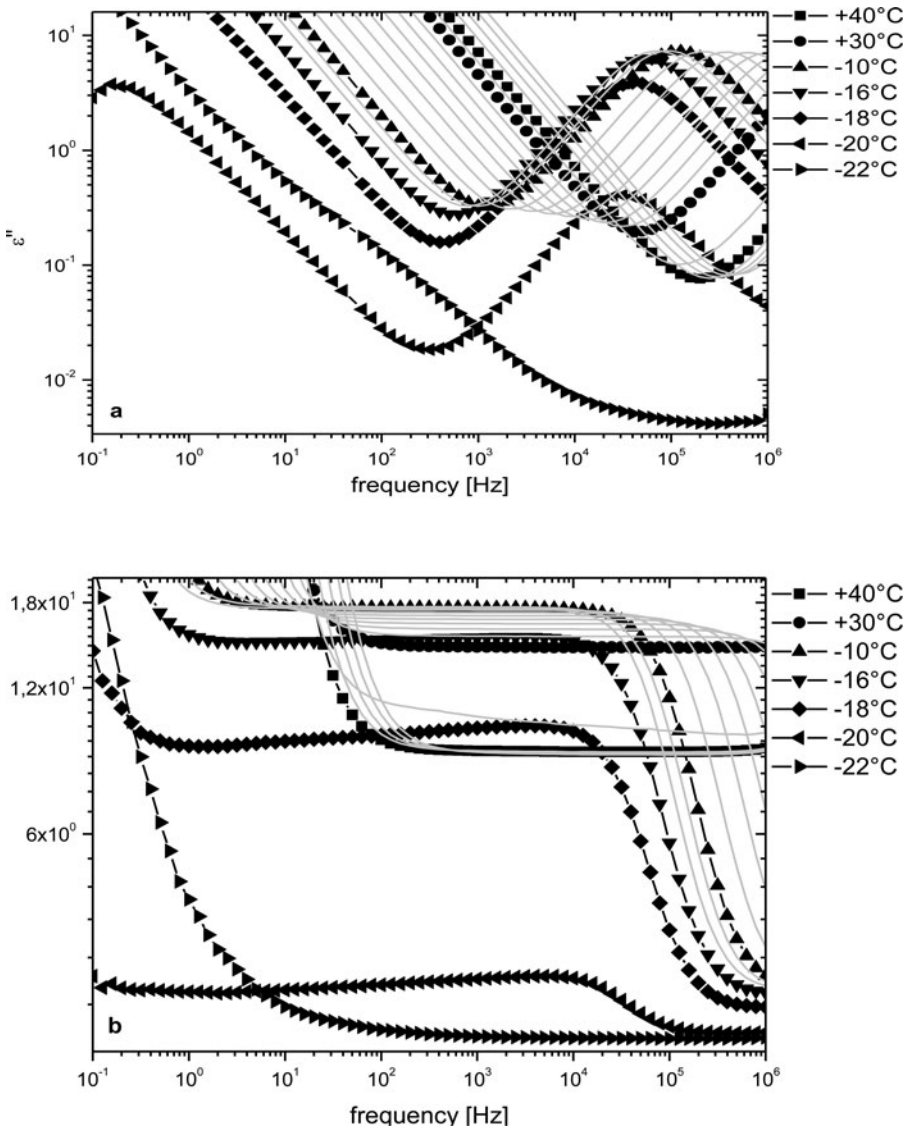

Figure 6. Imaginary and real part of dielectric function, ε'' and ε', as a function of frequency in a and b, respectively, at different temperatures, some of them indicated on the plots, for 5CB during cooling (experiment B)

rapidly from −18 to −20°C, whereas the relaxation disappears at the next temperature of −22°C, obviously due to crystallization (compare DSC results). The relaxation followed is the δ relaxation, as will be confirmed by analysis, whereas the α relaxation is at higher frequencies out of the range of measurements.

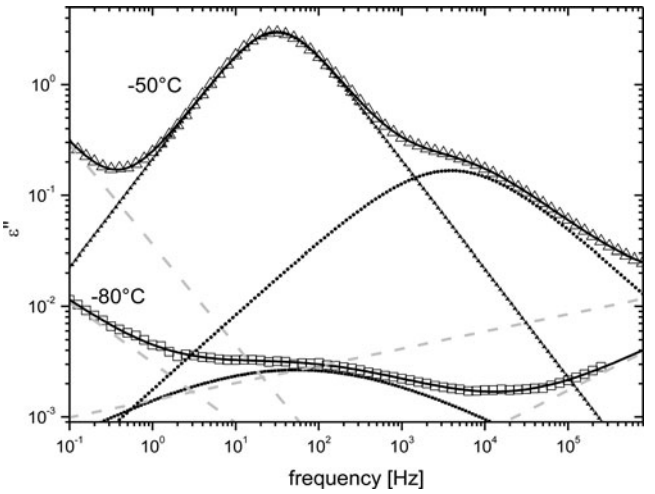

Figure 7. Frequency dependence of imaginary part of dielectric function, ε'', at -80°C and -50°C from experiment A. Fitting curves are shown. Squares: Cole-Cole function that describes β relaxation. Circles: Cole-Cole function that describes α relaxation. Up Triangles: Cole-Cole function that describes δ relaxation. Dashed lines: contributions of relaxations at lower and higher frequencies.

Molecular Mobility - Analysis

Information on the time scale, the relaxation strength and the shape of the relaxations were extracted by fitting the ε''vs frequency data with a sum of Cole-Cole terms (one or two terms depending on the number of relaxations present at each temperature in the frequency window of measurement) and exponential terms in order to take into account relaxations that are out of the frequency window [29]:

$$\varepsilon''(f) = \sum_{j=1}^{2} Im\left[\frac{\Delta\varepsilon_j}{1+\left(i\frac{f}{f_{max,j}}\right)^{a_j}}\right] + c_j f^{-n_j} \tag{1}$$

where $\Delta\varepsilon$ denotes the dielectric strength of the relaxation, α describes the symmetric broadening of the peak ($\alpha = 1$ for Debye) and f_{max} the frequency of the peak. The exponent n takes positive and negative values for relaxations at lower and higher frequencies, respectively.

In Figure 7 fitting curves are presented for -80°C and -50°C where the three relaxations observed in 5CB are in the frequency window of the measurement. Figure 8 shows results of the analysis for the time scale (Arrhenius plot, Fig. 8a) and for the dielectric strength of all the relaxations studied (Fig. 8b).

The temperature dependence of the relaxation rate of the β relaxation follows the Arrhenius equation [35]:

$$f_{max} = f_0 \cdot exp\left(-\frac{E_{act}}{kT}\right) \tag{2}$$

where f_0 denotes the relaxation rate at infinite temperature, E_{act} the activation energy and k the Boltzmann constant.

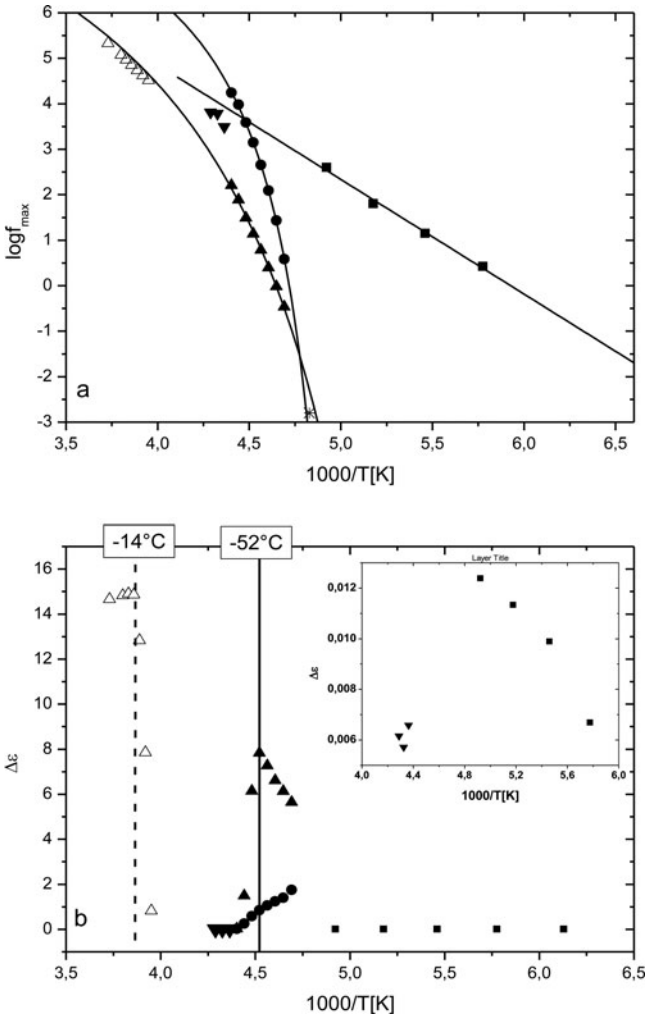

Figure 8. Arrhenius diagram (a) and dielectric relaxation strength, $\Delta\varepsilon$, as a function of inverse temperature (b) for all the dielectric relaxations observed, as came out from the fitting procedure. Full and open symbols are used for the experiments during heating (experiment A) and cooling (experiment B), respectively. The inset in b shows $\Delta\varepsilon$ for the β relaxation and for the weak relaxation in the crystalline sample in magnification. The lines in the Arrhenius diagram correspond to Arrhenius and VTF fittings. In the Arrhenius diagram the peak temperature of TSDC is included at the equivalent frequency of 1.6 mHz [7]. The vertical lines in b at -14 and -52°C are to guide the eye, details in text. Squares are for the β relaxation, circles for the α relaxation, up triangles for the δ relaxation, and down triangles for the weak relaxation in the crystalline sample.

The temperature dependence of the relaxation rate of the α and δ relaxations follows the Vogel-Tammann-Fulcher (VTF) equation [35]:

$$f_{max} = f_0 \cdot exp\left(-\frac{B}{T - T_0}\right) \tag{3}$$

where f_0 is a pre-exponential factor, B is a constant and T_0 is the so-called Vogel or ideal glass transition temperature, which is found to be 30–70 K below the thermal glass transition temperature.

The results of the analysis show that the β relaxation, which is reported for the first time in 5CB, is a symmetric relaxation with a shape parameter of 0.5 (eq. (1)), it follows Arrhenius behavior with an activation energy of 0.5 eV and a pre exponential factor of 10^{15}Hz, and its relaxation strength $\Delta\varepsilon$ increases with increasing temperature (inset to Fig. 8b). Regarding the origin of the β relaxation, some characteristics, in particular the increase of $\Delta\varepsilon$ with increasing temperature and the merging with the α relaxation, favor an explanation in terms of a Johari-Goldstein relaxation. Such a relaxation has been observed in many rigid amorphous glass formers and has been shown to bear a strong correlation to the α relaxation associated with the glass transition, being a precursor of that [33, 34]. More focused measurements in the region of and above T_g, combined with measurements on other cyanobiphenyls, are needed to further clarify the origin of the β relaxation measured in this work.

The β relaxation could not be followed by TSDC in the present work. This is not surprising, as extrapolation of the Arrhenius temperature dependence of Fig. 8a to the equivalent frequency of TSDC measurements of 1.6 mHz, corresponding to a relaxation time of 100s [7, 8], yields an expected peak temperature of the corresponding TSDC peak of about -130°C, which is out of the temperature range of TSDC measurements in this work. It is interesting to note, however, that no sub-glass relaxation was detected by TSDC measurements in 5CB down to -170°C in ref [13] and that the authors discussed this negative result in terms of the expected small strength of such a relaxation on the basis of the molecular structure of 5CB (as confirmed by the DRS results in Fig. 8b). This point will be further followed in future work by extending the temperature range of TSDC measurements to lower temperatures and by measuring more members of the cyanobiphenyl family, as mentioned above.

Coming now to the α relaxation, the results of the analysis show that this is a symmetric relaxation, which becomes narrower with increasing temperature, and follows a VTF behavior (with fitting parameters $f_0 = 10^9$Hz, B = 379K, T_0 = 194K), while its dielectric strength $\Delta\varepsilon$ decreases with increasing temperature almost linearly in the representation of Fig. 8b. The time scale of the relaxation does not change with crystallization at -52°C, whereas $\Delta\varepsilon$ decreases faster with increasing temperature in the region of crystallization. Work is in progress to follow in detail the evolution of time scale and strength of the α relaxation (and of the δ relaxation) with crystallization by combining isothermal DRS with time as a parameter and DSC measurements. The TSDC point is very close to the extrapolation of the VTF curve at low temperatures. Following the convention – definition of $T_{g,diel}$ by $\tau(T_{g,diel}) = 100$s [29, 33], this extrapolation yields $T_{g,diel} = -65^{\circ}$C, which is close to $T_g = -71^{\circ}$C by DSC (Fig. 1) and $T_m = -67^{\circ}$C by TSDC (Fig. 3). As mentioned in the Introduction, the α relaxation, studied by several investigators [18–26], has been assigned to different tumbling fluctuations of the 5CB molecule around its long axis.

The δ relaxation, observed during heating (experiment A) is a narrow symmetric relaxation with a shape parameter of 0.98, follows a VTF behavior (with fitting parameters $f_0 = 10^{10}$Hz, B = 1004K, T_0 = 172K), and its dielectric strength $\Delta\varepsilon$ increases linearly with decreasing inverse temperature (Fig. 8b). A sudden decrease of $\Delta\varepsilon$ is observed for T>-52°C (denoted by the vertical solid line in Fig. 8b) due to crystallization of the sample (which occurs at lower temperatures compared to DSC due to the different thermal protocol of DRS measurements – effectively lower heating rate), without any significant change of the time scale of the relaxation. Data from the cooling experiment (experiment B) follow

the VTF line at high frequencies (Fig. 8a, open symbols). When all the data are included in fitting, the following values for the parameters are obtained: $f_0 = 10^{9.4}$Hz, B = 886K, $T_0 = 174$K). The dielectric relaxation strength $\Delta\varepsilon$ is higher during cooling and exhibits a different temperature dependence compared to the one observed during heating. The lower values of $\Delta\varepsilon$ in the heating experiment can be explained, qualitatively at this stage, by the partial crystallization at about -25°C (Fig. 1) which occurs during cooling preceding the heating experiment. Work in progress mentioned above with respect to the α relaxation, combined DRS-DSC studies, will shed more light on that point. Adachi and coworkers discussed changes in ε' after a cooling-heating cycle in terms of possible changes in the orientation of the molecules with respect to the electrodes [23], a point worth to be followed in future work. Again a sudden decrease of relaxation strength is observed for $T > -14^\circ$C (denoted by the dashed line in Fig. 8b) due to crystallization of the sample, without any significant change of the time scale of the relaxation.

On approaching the glass transition region from high temperatures, the time scale of the α relaxation exhibits a steeper temperature dependence compared to the δ relaxation (Fig. 8a), resulting in higher T_0 temperature (Vogel temperature, eq. (3)) for the α than the δ relaxation, 194K against 172K (or 174K if we consider only the heating experiment). A similar observation was made by Bras et al. [20] in E7, which is a mixture of CB5 and three more molecular crystals. The TSDC results show only one process in the region of the glass transition, in agreement with recent TSDC results in 5CB [13]. It would be interesting in future work to fill the (not easily accessible) gap of measurements close to T_g (Fig. 8a), e.g. by slow time domain measurements, and follow the evolution and separation of α and δ out of the α relaxation, with respect to both time scale and strength of the relaxations. We note, with respect to strength of the relaxations, that $\Delta\varepsilon$ of both relaxations measured by DRS in the region of the glass transition (Fig. 8b) is significantly smaller than $\Delta\varepsilon$ of about 20 calculated from TSDC measurements for a sample polarized in the isotropic or the nematic phase (Fig. 3a). This could indicate a difference in the orientation of the molecules in the two experiments, due to the application of a relatively high dc polarizing field in TSDC measurements. Experiments are in progress to further follow this point.

In the DRS measurements during heating (experiment A, Fig. 5) only a very weak relaxation could be followed at temperatures higher than about -45°C, where the much stronger α and δ relaxations diminish due to crystallization of the sample. Results of the analysis for this relaxation have been included in Fig. 8 only three temperatures, where the relaxation could be followed. The trace of the time scale of the relaxation in Fig. 8a suggests a close relation to the β relaxation. Work is in progress on 5CB to verify this point, whereas measurements on more cyanobiphenyls would be much helpful in that respect.

Conclusions

Molecular dynamics in the molecular crystal 4-n-pentyl-4′-cyanobiphenyl (5CB) was investigated by broadband dielectric relaxation spectroscopy (DRS) and thermally stimulated depolarization currents (TSDC). The latter is a dielectric technique in the temperature domain, offering, among others, the possibility to extend measurements to lower frequencies, not easily accessible by DRS. Next to the supercooled nematic phase, where the two well-known α and δ relaxations were followed, assigned to reorientation of the molecule around its short axis and to different tumbling fluctuations of the molecule around its long axis, respectively, measurements in the present study were extended to lower temperatures in the glassy state, where a weak sub-glass β relaxation was observed and studied. The relaxations were analyzed in terms of time scale, strength and shape by fitting model functions to the

data. The time scale of the β relaxation is described by the Arrhenius equation, whereas that of the α and δ relaxations by the VTF equation, characteristic for cooperative processes. The traces of the two relaxations approach each other and cross in the glass transition region. Several issues remain open or arose from the present study, such as the character and the origin of the sub-glass β relaxation and its relation to a weaker process at higher temperatures in the highly crystalline material, and the interplay of the α and δ relaxations in the glass transition region. These issues should be further investigated in future work, comparative measurements on selected cyanobiphenyls being particularly important in that respect.

In addition to studying molecular dynamics, isochronal DRS and TSDC measurements were used to follow phase transitions in 5CB, in comparison with DSC, by taking advantage of the different values of the real part of dielectric function ε' in the different phases and of the thermodielectric effect, respectively. The results demonstrate the power of dielectric techniques, in particular TSDC, for monitoring phase transitions in liquid crystals, as confirmed also by TSDC measurements under different polarization conditions in CE8, a molecular liquid crystal with a rich phase sequence. This point is worth to follow in future work.

Acknowledgments

This research has been co-financed by the European Union (European Social Fund, ESF) and Greek national funds through the Operational Program "Education and Lifelong Learning" of the National Strategic Reference Framework (NSRF). Research Funding Program: THALES.

References

[1] Moscicki, J. K. (1992). In: *Liquid Crystal Polymers: From Structures to Applications*, Collyer, A. A. (Ed.), Chapter 4, Elsevier: London, 143.
[2] Williams, G. (1993). In: *Materials Science & Technology Series*, Thomas, E. L. (Ed.), VCH Publications: Weinheim, Vol. 12, 471.
[3] Simon, G. P. (1997). In: *Dielectric Spctroscopy of Polymeric Materials: Fundamentals and Applications*, Runt, J. P. & Fitzgerald, J. J. (Eds.), Chapter 12, American Chemical Society: Washington, DC, 329.
[4] Kremer, F. & Schoenhals, A. (2003). In: *Broadband Dielectric Spectroscopy*, Kremer, F. & Schoenhals, A. (Eds.), Chapter 10, Springer: Berlin, 385.
[5] Nordio, P. L., Rigatti, G. & Segre, U. (1973). *Mol. Phys.*, *25*, 129.
[6] Williams, G. (1994). In: *The Molecular Dynamics of Liquid Crystals*, Luckhurst, G. R. & Veracini, C. A. (Eds.), Chapter 17, Kluwer Academic: Dordrecht, 431.
[7] van Turnhout, J. (1980). In: *Electrets, Topics in Applied Physics, Vol. 33*, Sessler, G. M. (Ed.), Chapter 3, Springer: Berlin, 81.
[8] Fragiadakis, D. & Pissis, P. (2007). *J. Non-Cryst. Solids*, *353*, 4344.
[9] Neagu, E., Neagu, R., Daly, W. H. & Negulescu, I. I. (1993). *IEEE Trans. Electr. Insul.*, *28*, 122.
[10] Suarez, N., Laredo, E., Bello, A., Gomez, M. A., Marco, C. & Fatou, J. M. C. (1996). *Polymer*, *37*, 3207.
[11] Moura Ramos, J. J. & Mano, J. F. (1996). *Thermochim. Acta*, *285*, 547.
[12] Nikonorova, N., Borisova, T., Barmatov, E., Pissis, P. & Diaz-Calleja, R. (2003). *Macromolecules*, *36*, 5784.
[13] Moura Ramos, J. J. & Diogo, H. P. (2013). *Mol. Cryst. Liq. Cryst.*, *571*, 19.
[14] Schober, W. & Fischer, F. (1983). *Mol. Cryst. Liq. Cryst.*, *100*, 167.

[15] Dantras, E., Dandurand, J., Lacabanne, C., Laffont, L., Tarascon, J. M., Seguy, I., Destruel, P., Bock, H. & Fouet, S. (2004). *Phys. Chem. Chem. Phys.*, *6*, 4167.
[16] Charnetskaya, A. G., Polizos, G., Shtompel, V. I., Privalko, E. G., Kercha, Y. Y. & Pissis, P. (2003). *Eur. Polym. J.*, *39*, 2167.
[17] liqcryst.lci-publisher.com
[18] Urban, S., Gestblom, B. & Dabrowski, R. (1999). *Phys. Chem. Chem. Phys.*, *1*, 4843.
[19] Drozd-Rzoska, A. (2009). *J. Chem. Phys.*, *130*, 234910.
[20] Bras, A. R., Dionisio, M., Huth, H., Schick, Ch. & Schoenhals, A. (2007). *Phys. Rev. E*, *75*, 061708.
[21] Massalska-Arodz, M., Williams, G., Smith, K., Conolly, C., Aldridge, G. A. & Dabrowski, R. (1998). *J. Chem. Soc. Faraday Trans.*, *94*, 387.
[22] Kundu, S. K., Okudaira, S., Kosuge, M., Shinyashiki, N. & Yagihara, S. (2008). *J. Chem. Phys.*, *129*, 164509.
[23] Hori, H., Urakawa, O. & Adachi, K. (2004). *Macromolecules*, *37*, 1583.
[24] Rozanski, S. A., Kremer, F., Groothues, H. & Stannarius, R. (1997). *Mol. Cryst. Liq. Cryst.*, *303*, 319.
[25] Sinha, G., Leys, J., Glorieux, C. & Thoen, J. (2005). *Phys. Rev. E*, *72*, 051710.
[26] Grigoriadis, C., Duran, H., Steinhart, M., Kappl, M., Butt, H.-J. &Floudas, G. (2011). *ACS Nano*, *5*, 4208.
[27] Gross, B. (1954). *Phys. Rev.*, *94*, 1545.
[28] Pissis, P. & Apekis, L. (1991). *J. Non-Cryst. Solids*, *131-133*, 95.
[29] Kremer, F. & Schoenhals, A. (Eds). (2003). *Broadband Dielectric Spectroscopy*, Springer: Berlin.
[30] Papadopoulos, P., Grigoriadis, C., Haase, N., Butt, H.-J., Muellen, K. & Floudas, G. (2011). *J. Phys. Chem. B*, *115*, 14919.
[31] Klonos, P., Pandis, C., Kripotou, S., Kyritsis, A. & Pissis, P. (2012). *IEEE Trans. Diel. Electr. Insul.*, *19*, 1283.
[32] Cava, R. J., Patel, J. S., & Rietman, E. A. (1986). *J. Appl. Phys.*, *60*, 3093.
[33] Johari, G. P. & Goldstein, M. (1970). *J. Chem. Phys.*, *53*, 2372.
[34] Kessairi, k., Capaccioli, S., Prevosto, D., Lucchesi, M., Sharifi, S. &Rolla, P. A. (2008). *J. Phys. Chem. B*, *112*, 4470.
[35] Donth, E. (2001). *The glass transition: relaxation dynamics in liquids and disordered materials*, Springer: Berlin.